Scale invariance in coarsening of binary and ternary fluids

K. C. Lakshmi* and P. B. Sunil Kumar†
Department of Physics, Indian Institute of Technology Madras, Chennai 600 036, India
(Received 22 July 2002; published 29 January 2003)

Phase separation in binary and ternary fluids is studied using a two-dimensional lattice gas automata. The lengths given by the the first zero crossing point of the correlation function and the total interface length is shown to exhibit power law dependence on time. In binary mixtures, our data clearly indicate the existence of a regime having more than one length scale, where the coarsening process proceeds through the rupture and reassociation of domains. In ternary fluids; in the case of symmetric mixtures there exists a regime with a single length scale having dynamic exponent 1/2, while in asymmetric mixtures our data establish the break down of scale invariance.

DOI: 10.1103/PhysRevE.67.011507 PACS number(s): 64.75.+g, 47.55.Kf, 47.55.−t, 47.11.+j

I. INTRODUCTION

A mixture of fluids phase separate into domains when quenched below its critical temperature. Since many systems of scientific and technological interest are multicomponent mixtures, the phase behavior of fluid mixtures are of current interest. The equilibrium state of incompatible fluids is one in which the pure phases are separated by a single connected interface. However, in the thermodynamic limit, starting from a mixed phase this equilibrium is never reached. In view of this, the kinetics of the phase separation process gains importance.

In the case of phase separating binary fluids, experiments [1–4] and numerical simulations [5–7] have clearly established the importance of hydrodynamics in the determination of late time domain growth laws. In spite of all efforts, a complete theoretical understanding of this highly nonlinear phenomena remains unsolved [8]. This is mainly due to the fact that studying kinetics of liquid phase separation involves the solution of mutually coupled equations; the Navier-Stokes equation for the flow and the equation of continuity for the order parameter.

Early experimental and theoretical studies of these binary fluid systems, assume that there exists, at late times, a dynamical scaling regime exhibiting similar behavior under an appropriate rescaling of time and length scales. Dynamical scaling is characterized by the single time-dependent length scale $R(t)$. The domain growth follows a simple and generic algebraic form, $R(t) \propto t^{\alpha}$, where α represents the exponent characteristic of the universality class to which the system belongs. Scaling and dimensional analysis by Siggia [9], Furukawa [10], San Miguel [11], and more recently by Bray [8] addresses this question of the growth exponent taking this length scale $R(t)$ to be the average size of the ordering domains. In two dimensions, in the case of minority B phase separating from a A rich mixture, the domains coarsen via evaporation-condensation process leading to the exponent $\alpha = 1/3$. The late time growth is governed by droplet coalescence leading to the exponent $\alpha = 1/2$. In the case of symmetric binary mixtures, thermal fluctuations can drive the initial $\alpha = 1/3$ regime to a $\alpha = 1/2$ regime [11]. Most of the studies, however, show a crossover from the $\alpha = 1/3$ to an inertial $\alpha = 2/3$ regime predicted by Furukawa [10].

More recently many researchers have pointed out the absence of scaling in two-dimensional phase separating fluids. It is shown that competition between diffusive and hydrodynamic growth leads to breakdown of scale invariance in symmetric binary fluids [12]. In the viscous hydrodynamic regime, scaling is observed only in the case of coarsening through coalescence. Even after starting from a droplet state one can enter a bicontinuous state by coalescence induced coalescence mechanism [13] leading to a breakdown of scaling. Alternatively, starting from a droplet state scaling is maintained, in symmetric binary mixtures, if the droplet morphology is self-sustaining [14]. In the inertial hydrodynamics regime, full scaling is recovered [14,15]. Excellent scaling is observed also in the crossover regime from the viscous hydrodynamic to the inertial hydrodynamic regime [16].

Variety of techniques have been used to simulate growth kinetics in the binary immiscible fluids. Direct simulations of model H have been used to study the domain growth and scaling using various defined length scales [8,15]. Lattice Boltzmann simulations have been particularly useful in exploring the late time hydrodynamic regime [17–19]. One problem with this technique is that it does not include thermal fluctuations. On the other hand thermal fluctuations are inherent in lattice-gas models. Rothman and Keller proposed a lattice-gas model (RK model) for the binary immiscible fluids [20]. This model has been used for simulating 2D binary fluid phase separation at different overall fluid densities [21,22].

Though most of the techniques mentioned in the previous paragraph have been extended to study a mixture of two fluids and a surfactant [22–24], our understanding of phase separation wherein all three are fluid components is rather limited. Molecular dynamics simulations by Laradji *et al.* [25] seem to indicate that hydrodynamic flow is not likely to control the separation process in ternary fluid system. This study indicates that the ternary system at late times reaches a dynamical scaling regime during which the domains show a growth law $R(t) \propto t^{1/3}$, in agreement with the classical theory of Lifshitz and Slyozov. Gunstensen and Rothman extended

*Email address: lakshmi@physics.iitm.ac.in
†Email address: sunil@physics.iitm.ac.in

the lattice-gas model (GR Model) to study ternary immiscible fluids [26] but do not make any comments about the dynamical exponents. In this model, the total energy function is the sum of the work done by the ''color flux'' $\vec{f}_i$ of each component against its ''color field'' $\vec{Q}_i$ and is given by $W = \Sigma \sigma_i \vec{f}_i \cdot \vec{Q}_i$. More recently, a level set method was proposed for the study of phase separation in fluid mixtures [27]. In this method one assumes convective terms to dominate the coarsening; local volume fraction function $\phi_i(x,t)$ of the components is then coupled to the local velocity field $\vec{v}$ through the kinetic equation

$$\frac{\partial \phi}{\partial t} = -\vec{v} \cdot \vec{\nabla} \phi. \tag{1}$$

The fluid velocity $\vec{v}$ satisfies Navier-Stokes equation

$$\frac{\partial \vec{v}}{\partial t} + (\vec{v} \cdot \vec{\nabla})\vec{v} = \nu \vec{\nabla}^2 \vec{v} - \frac{\vec{\nabla} P}{\rho} - \frac{\vec{F}}{\rho}, \tag{2}$$

where, P is the pressure, ν is the kinematic viscosity, and ρ is the density. The interfacial energy between the domains enters the equations only through the external force $\vec{F}$;

$$\vec{F} = \sum_{i=A,B,C} \sigma_i' \, \delta(\phi_i) \kappa(\phi_i) \hat{\mathbf{n}}, \tag{3}$$

where $\kappa(\phi_i)$ is the curvature of the ϕ_i domain interface, σ is the surface tension defined such that for the AB interface the surface tension is $\sigma_A^i + \sigma_B^i$.

The zero contour of the function ϕ_i specifies the interface of the domains. Immiscible three-component mixtures with majority components A and B having the same volume fraction and a minority C phase was studied using this method [27]. They find a power law dependence of interface length with dynamic exponents in the range 0.5–0.6.

In this paper, we discuss lattice-gas simulations of the binary and ternary mixtures phase separating in two dimensions. We calculate cluster size distribution, total interface length, and the density density correlation functions for each of the components. We see that, in some cases, the interface length and the first zero of the correlation function; though shows power law dependence on time, do not have the same dynamic exponents, thus, violating scaling.

In binary mixtures, large difference in the parameters σ_i of the two components can lead to breakdown of scaling with the domains coarsening through rupture and coalescence. In the symmetric ternary mixtures with equal σ_i and equal volume fractions, we see the average size of the ordering domains, $R(t) \propto t^{1/3}$ in agreement with the results reported earlier. At late times, we observe a crossover to a $t^{1/2}$ regime which is not reported in previous simulations. As we reduce the volume fraction of one of the components this exponent changes to 2/3, consistent with the inertial regime in two-component mixtures. In the asymmetric case; wherein one of the component is miscible in the other two, we observe a $R(t) \propto t^{1/2}$ and a crossover to $t^{2/3}$ as the volume fraction of the solute is reduced to zero.

By choosing a substrate which has minimum interaction with the fluid one should be able to conduct experiments on fluid separation problem in two dimensions. Such quasi-two-dimensional geometries have been used for studying three-fluid phase separation [4].

The paper is organized as follows: In Sec. I, we introduce the problem and summarize previous results. A detailed account of the lattice-gas automaton model and the algorithm for computing the cluster size and interface length are given in Sec. II. Next, we discuss the results of our simulations on the binary fluids. Section IV deals with the symmetric and asymmetric ternary fluids. In Sec. V, we conclude the paper with a summary of the results.

II. THE MODEL

Lattice-gas automaton is an alternative numerical description of fluid flow dynamics. This model approximates reality by constraining motions and collisions of fluid particles to a lattice, where each particle represents a finite mass of fluid. Lattice-gas automaton models represent, in the continuum, the incompressible Navier-Stokes equation correctly and are extensively used in simulations of fluids.

In this paper, we discuss simulations using the Frisch, Hasslacher, and Pomeau (FHP) model for fluids. Much has been written about the FHP model, which was first introduced in 1986 by Frisch, Hasslacher, and Pomeau [28]. The fully discrete microscopic dynamics of the FHP model maps into the macroscopic behavior of hydrodynamics. A modified version of the FHP model for immiscible fluid was introduced by Rothman and Keller [20]. In this model, which is defined on a hexagonal lattice, particles at the lattice sites are allowed to take seven possible velocities, $\vec{c}_i$, $i \in \{0,1,2,3,4,5,6\}$. Boolean variables indicate the occupation number at a particular site at a given time. The dynamics is such that no more than one particle enters the same site at the same time with the same velocity; the exclusion principle. The particles undergo collision that conserves, at every site, the total number of particles, their total momentum, and the total kinetic energy after each time step.

Multiphase flows in which different species of fluids coexist, move and interact are an important domain of application of the lattice-gas approach. Models for miscible, immiscible, and reactive flows have been proposed. Interaction between the species are the key ingredient of multiphase flows and depending on the nature of the physical processes, different interactions will be considered.

The lattice-gas approach has the important advantage that the interface between the different fluids appear, naturally, as a consequence of the way the fluids are modeled in terms of particles. In this paper, we represent the different phases by assigning the particles a ''color.'' Now the state of any vertex at $\vec{r}$ is specified by a total density vector $\vec{\phi}(\vec{r})$ and the color vectors $\vec{q}_i(\vec{r})$ with Boolean variables ϕ_j and q_{ij} as the components of this vector. In the case of ternary mixtures, i can take three values $+1$, -1, and 0. This is illustrated clearly in Fig. 1. We define the average density as the ratio of total number of particles to the maximum number of particles

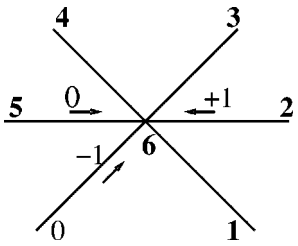

FIG. 1. The *state* of a lattice point is given by the vectors $\vec{\phi}=\{1,0,1,0,0,1,0\}$, $\vec{q}_1=\{0,0,1,0,0,0,0\}$, $\vec{q}_{-1}=\{1,0,0,0,0,0,0\}$, and $\vec{q}_0=\{0,0,0,0,0,1,0\}$.

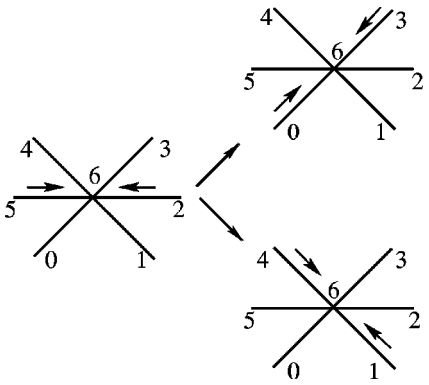

FIG. 2. Possible configurations in a two-particle collision.

possible. This is given by $d=\Sigma_{i=0,j=1}^{i=6,j=N}\phi_i(r_j)/(7N)$, where N is the total number of sites in the lattice.

Drawing analogies from electrodynamics, we define a color flux and color field at every lattice point for each type of particles. In the case of ternary mixture the color flux at a lattice site is given by

$$\vec{Q}_1(\vec{r})=\sum_{j=0}^{j=5}\vec{c}_j q_{1j}, \tag{4}$$

$$\vec{Q}_{-1}(\vec{r})=\sum_{j=0}^{j=5}\vec{c}_j q_{-1j}, \tag{5}$$

$$\vec{Q}_0(\vec{r})=\sum_{j=0}^{j=5}\vec{c}_j q_{0j}. \tag{6}$$

And the local color gradients or fields are defined to be

$$\vec{f}_1(\vec{r})=\sum_{j=0}^{j=5}\vec{c}_j\sum_{k=0}^{k=6} q_{1k}(\vec{r}+\vec{c}_j), \tag{7}$$

$$\vec{f}_{-1}(\vec{r})=\sum_{j=0}^{j=5}\vec{c}_j\sum_{k=0}^{k=6} q_{-1k}(\vec{r}+\vec{c}_j), \tag{8}$$

$$\vec{f}_0(\vec{r})=\sum_{j=0}^{j=5}\vec{c}_j\sum_{k=0}^{k=6} q_{0k}(\vec{r}+\vec{c}_j). \tag{9}$$

Following the GR model, we write the work done by the flux against the field to be

$$W=-[\sigma_1\vec{f}_1(\vec{r})\cdot\vec{Q}_1(\vec{r})+\sigma_{-1}\vec{f}_{-1}(\vec{r})\cdot\vec{Q}_{-1}(\vec{r}) +\sigma_0\vec{f}_0(\vec{r})\cdot\vec{Q}_0(\vec{r})], \tag{10}$$

where σ_i are the parameters which determine the surface tension between different phase boundaries. The three phases are labeled by $i=\pm 1,0$.

The simulation proceeds in two steps, collision and translation. During the collision process, particles at a given lattice site can exchange their velocity and color. The collision rules are such that the work performed by the flux against the field is minimized, subject to the constraints of the exclusion principle as well as the principles of mass, momentum, and particle conservation. There can be a number of configurations which satisfy the above constraints, and in principle one should pickup that configuration which minimizes energy from this full set of possible configurations. In practice only a ''limited'' number of configurations are considered. In our simulations, we take into account the following possibilities.

If a site has more than three particles or if their total momentum is nonzero, then we pickup all possible pairs and an attempt is made to exchange their colors. The exchange is accepted only if it lowers the energy.

When two particles occupy the same site with opposite velocities there are two cases to consider. In one, both the particles are of the same color. Then a rotation of the configuration by $0°$, $60°$, or $120°$ is attempted as shown in Fig. 2. The other possibility is that the two are of different colors. Then, we need to check the possibilities for $0°$, $\pm 60°$, $\pm 120°$, and $180°$ rotation.

When three particles collide at an angle of $120°$, there are three possibilities. When all the particles have the same color, they could just reverse their directions or retain their velocities. When the colors are not the same, similar to two-particle collisions, the configuration could now be rotated by 0, ± 60, ± 120, and 180. In all the above cases, the lowest energy configuration is chosen as the final state.

There is one special case of three-particle collision in which two particles have opposite velocities and the third one is a zero velocity particle. In this case, apart from rotating the configuration an exchange of color between pairs is also attempted.

Next step in the simulation is the translation in which all particles are moved in the direction of their velocities. This collision and translation process completes one time step.

To understand the various competing terms in this model, we first look at a two-component fluid mixture and introduce the variables $q_k=q_{1k}-q_{-1k}$, $\phi_k=q_{1k}+q_{-1k}$, in the direction k. The two components are now designated by $q_k=\pm 1$. Substituting these variables in the equations for $\vec{f}_1,\vec{f}_{-1}$ and $\vec{Q}_1,\vec{Q}_{-1}$, we can obtain from Eq. (10) the work done to be

$$W = -(\sigma_1 \vec{f}_1 \cdot Q_1 + \sigma_{-1} \vec{f}_{-1} \cdot \vec{Q}_{-1}$$
$$= -\Bigg[\sum_k \vec{c}_k q_k \cdot \Bigg((\sigma_1 + \sigma_{-1}) \sum_i \vec{c}_i \sum_l q_l \Big(\vec{r} + \vec{c}_i$$
$$+ (\sigma_1 - \sigma_{-1}) \sum_i \vec{c}_i \sum_l \phi_l (\vec{r} + \vec{c}_i) \Bigg)$$
$$+ \sum_k \vec{c}_k \phi_k \cdot \Bigg((\sigma_1 + \sigma_{-1}) \sum_i \vec{c}_i \sum_l \phi_l (\vec{r} + \vec{c}_i)$$
$$- (\sigma_1 - \sigma_{-1}) \sum_i \vec{c}_i \sum_l q_l (\vec{r} + \vec{c}_i) \Bigg) \Bigg]. \quad (11)$$

Momentum conservation implies that the last two terms in the above equation do not contribute to the dynamics. The first term decides the energy of the interface between the two phases. The second term favors movement of particles toward higher or lower densities depending on their color. For example, when $\sigma_1 - \sigma_{-1} > 0$ this terms imply higher diffusivity of particles with $q = -1$. Thus, increasing $|\sigma_1 - \sigma_{-1}|$ is like increasing the ''temperature.''

The earlier lattice-gas model for two-component fluids by Rothman and Keller used $\sigma_1 = \sigma_{-1} = \sigma$. In this model the work done is given by

$$W = -\sigma \vec{f} \cdot \vec{Q}, \quad (12)$$

where $\vec{Q}(\vec{r}) = \Sigma_{j=0}^{j=5} \vec{c}_j q_j$ and $\vec{f}(r) = \Sigma_{j=0}^{j=5} \vec{c}_j \Sigma_{k=0}^{k=6} q_k (\vec{r} + \vec{c}_j)$. We can then introduce thermal fluctuation by defining an inverse temperature like parameter β such that the new configuration at every time step is accepted with a probability proportional to $\exp -\beta (W_{old} - W_{new})$ [22]. Unless specified, otherwise, the results discussed in this paper are obtained using the GR model.

Correlation functions and domain distribution functions

We define the pair correlation functions

$$C_{ij}^q (\vec{r}, t) = \Big\langle \sum_k q_{i,k} (\vec{x}, t) \sum_k q_{j,k} (\vec{x} + \vec{r}, t) \Big\rangle$$
$$- \Big\langle \sum_k q_{i,k} (\vec{x}) \Big\rangle \Big\langle \sum_k q_{j,k} (\vec{x}) \Big\rangle, \quad (13)$$

$$C_{ij}^h (\vec{r}, t) = \langle h_i (\vec{x}, t) h_j (\vec{x} + \vec{r}, t) \rangle - \langle h_i (\vec{x}) \rangle \langle h_j (\vec{x}) \rangle, \quad (14)$$

Here, the subscripts i, j represent the color of the particles with $i, j = \pm 1, 0$. Field values h_i determines the *phase* at every lattice points. A lattice point belongs to the ith phase if h_i has a value higher than the other two. This means that most of the particles there belong to the ith color. We calculate the length $R_{ij}(t)$ as the first zero of the correlation function C_{ij}^h.

For the immiscible case wherein all three phases have the same surface tension, to calculate the border length and cluster size of the domains of a particular phase, say *A*, we use the following algorithm.

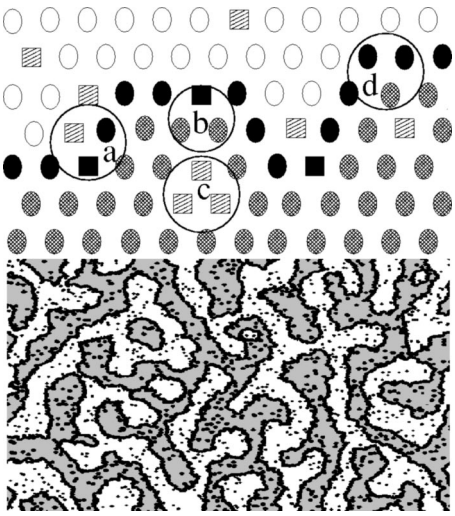

FIG. 3. (Top) Rules for determining the border. Squares represent *C* phase, open circles represent *B* phase, and the hashed circles represent *A* phase. The dark squares and circles are the border sites between the *A*-*C* phase and the *B*-*C* phase. (Bottom) Snapshot from the simulation of ternary fluid with one component miscible in the other two. The dark regions are the border between the *A*-*C* (white) and *B*-*C* (gray) domains.

All lattice sites are picked sequentially. If a particular site belongs to the phase *A* and is not assigned a cluster number we give it a new number. All the neighbors of this site are then checked. If the neighbor belongs to the phase *A*, three possibilities arise. In one, the site does not have an assigned cluster number. We will then give this neighbor the same cluster number as the present site. In the second case, the neighbor has a number which is the same as the site . Here, we do not have to do anything more. In the third case, the neighbor has a number which is different from that of the present site. That is, the neighbor belongs to a different cluster. In that case, the clusters are merged by assigning smaller of the two numbers to all sites in the two clusters. A lattice site which belong to a particular phase is a border site if one of its neighbors is of a different phase.

In the case, wherein one of the phases is equally miscible in the other two; for example, let us consider *C* miscible in *A* and *B*, we have two phases, the *A*-*C* phase and the *B*-*C* phase, see Fig. 3. To label the domains, we then follow the same procedure as before. Any site belongs to the *A*-*C* phase if it is an *A* site or a *C* site whose neighbors are all *A* or *C*. For example, region *c* in Fig. 3 belongs to the *A*-*C* phase. The border of the *A*-*C* domain could be a *A* or *C* site. If it is an *A* site, it should have at least one *B* neighbor (region *d* in Fig. 3) or a *C* neighbor with the next nearest neighbor as *B* (region *a* in Fig. 3). If the border site belongs to the *C* phase then it should either have a neighbor which is a *B* site (region *b* in Fig. 3) or a *C* neighbor with the next nearest neighbor as *B* (region *a* in Fig. 3).

In the simulations, to prepare the initial configuration a particle is placed at a randomly chosen site. The velocity of the particle is chosen randomly from the seven possible directions such that the total momentum summed over all particles is zero. The color of the particle is again assigned

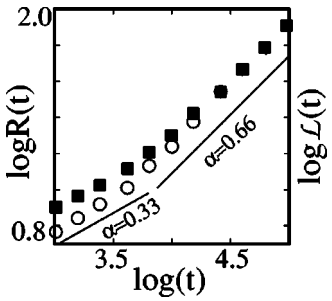

FIG. 4. The first zero of the correlation function R (open circles) and the total border length $\mathcal{L}$ (filled squares) for a binary fluid, with $\sigma_1=\sigma_{-1}=1$, with $\log_{10}$ (time). The average density of the fluids is $d=0.55$. The curves are shifted to make the comparison easy. Continuous lines with slope 2/3 and 1/3 are given as a guide to the eye.

randomly depending on the volume fraction of each component. Once the initial configuration is prepared the ensuing dynamics conserved the total number of particles, the net momentum, the total kinetic energy, and the volume fraction of each components.

Simulations are performed on a triangular lattice with 360 000 lattice points with periodic boundary conditions. The results are averaged over ten initial configurations. The dynamic exponents are obtained by a power law fit over one decade in time.

III. TWO-COMPONENT FLUIDS

In this section, we reexamine the well studied case of binary fluid coarsening following a critical quench. The fluids are labeled by $i=\pm 1$. Let us first look at the case $\sigma_1=\sigma_{-1}=1$. The time dependence of average domain size $R(t)$ which scales the same way as R_{ij} is shown in Fig. 4. At early time, we see Lifshitz-Slyozov-Wagner (LSW) $t^{1/3}$ [8] growth. At late times the growth of domains is controlled by the inertial hydrodynamics and we have the well known $t^{2/3}$ growth law [8].

To check for scaling, we compare the length R given by the first zero of the correlation function with the total border length $\mathcal{L}(t)$. As can be seen from Fig. 4, at late time, in the inertial hydrodynamic regime, the length $\mathcal{L}$ also exhibits power law dependence with a dynamic exponent 2/3. This agrees with earlier studies on binary fluid phase separation

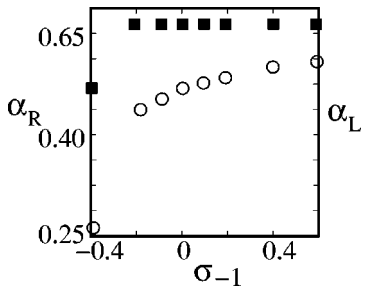

FIG. 5. Dynamic exponents of α_R and $\alpha_{\mathcal{L}}$ as a function of σ_{-1} for $\sigma_1=1$. The open circles represent $\alpha_{\mathcal{L}}$ and the dark squares represent α_R.

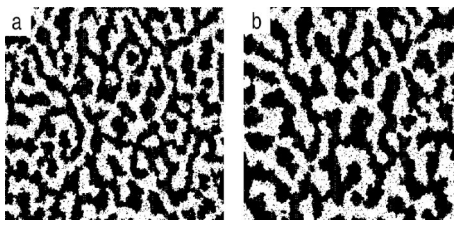

FIG. 6. Time evolution of binary mixture for $d=0.55$, $\sigma_1=1.0$, $\sigma_{-1}=-0.4$. The snapshots are taken at (a) $t=25\,118$ and (b) $t=39\,810$.

which predict scaling to hold in the inertial regime [14,15].

We now investigate the more general case of $\sigma_1\neq\sigma_{-1}$ with $\sigma_{-1}<\sigma_1$. The dynamic exponents α_R and $\alpha_{\mathcal{L}}$ characterizing the time dependence of R and $\mathcal{L}$ seem to vary differently with $\sigma_1-\sigma_{-1}$. This is depicted in Fig. 5. This results imply break down of scaling at lower values of σ_{-1}. The absence of scaling is clearly manifested in the snapshots given in Fig. 6, the coarsening process is through the breaking and joining of domains. Since the length $R(t)$ is decided by the big clusters it has a dynamical exponent characteristic of coalescence. On the other hand, the total border length $\mathcal{L}(t)$ has significant contribution from the small clusters which coarsen through evaporation condensation.

Similar change in the dynamical exponents of R was observed as a function of the inverse temperature like parameter β in the RK model [22]. For low β values the coarsening mechanism is very similar to that operating in the case of $\sigma_1\neq\sigma_{-1}$ in the GR model. This is shown in Fig. 7. The β dependence of α_R and L shown in Fig. 8 confirms absence of scaling. These exponents indicate the presence of more that one coarsening mechanism operating at the late time regime.

In the case of two-fluid mixtures with unequal volume fraction, we see the initial LSW regime crossing over to the $\alpha=1/2$ regime controlled by the droplet coalescence mechanism. The first zero of the correlation function R and the total border length $\mathcal{L}$ in this regime seems to indicate existence of simple scaling [18].

IV. THREE-COMPONENT FLUIDS

In this section, we look at two separate cases of phase separating three-component fluids. In one, we consider a *symmetric ternary mixture* with all the components having equal volume fraction and with the parameters σ_i in Eq. (10) set to $\sigma_1=\sigma_{-1}=\sigma_0$. This amounts to having the same sur-

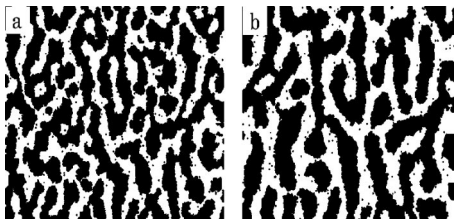

FIG. 7. Time evolution of binary mixture in the RK model for $d=0.55$, $\sigma=1.0$, $\beta=0.03$. The snapshots are taken at (a) $t=25\,118$ and (b) $t=39\,810$.

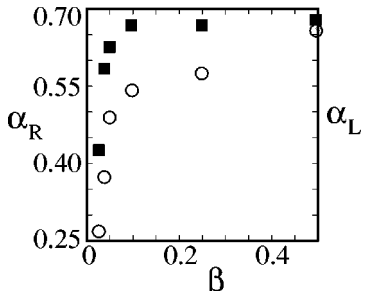

FIG. 8. Dynamic exponents of α_R and $\alpha_{\mathcal{L}}$ as a function of β for $\sigma=1$ in the RK model. The open circles represent $\alpha_{\mathcal{L}}$ and the dark squares represent α_R.

face tension for the $A-B, B-C$, and $A-C$ interfaces. The other case of interest is the *asymmetric mixture*, where we choose the parameters to be $\sigma_1=\sigma_{-1}$ and $\sigma_0<2(\sigma_1+\sigma_{-1})$. This choice of parameters ensures that one of the components (*solute*) is equally soluble in the other two. We will now discuss these two cases in detail.

1. Symmetric case

Starting from the mixed state, the symmetric ternary mixture, when quenched below the transition temperature, evolves to form droplets of individual components. Snapshots from the simulation, shown in Fig. 9, clearly establish the existence of sharp interfaces between the components. The first zero of correlation function R and the interface length $\mathcal{L}$ are plotted in Fig. 10 as a function of time.

Initial regime corresponds to the formation of droplets. In Fig. 10, we see a region with $R(t)\sim t^{1/2}$, where this droplets coalesce to form bigger domains. If the late time growth is due to the coalescence by droplet diffusion, as it is believed to be, then the following simple argument shows that the exponent should be 1/2.

If R is the typical radius of a droplet, we have the droplet number density $n\sim v/R^2$, where v is the volume fraction of the components in two dimensions. The time for a droplet to diffuse a distance of order of its radius is $t_R=R^2/D$, where D is the diffusion coefficient. The area swept out by the drop in time t (for $t>t_R$) is of the order $R^2t/t_R\sim Dt$. If t_c is the coalescence time, the expected number of drops in an area Dt_c is of the order unity, which means $nDt_c=1$. Since in two dimensions, the diffusion coefficient, $D\sim k_BT/\eta$, does not have any dependence on the droplet size,

$$tc\sim\frac{R^2}{vD}\sim\frac{\eta R^2}{vk_BT}. \tag{15}$$

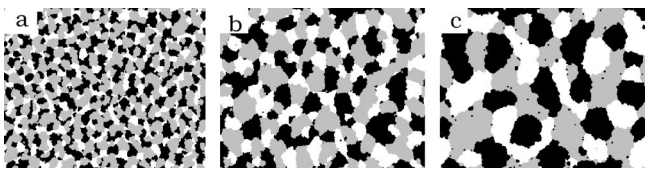

FIG. 9. Time evolution of three-fluid mixture for $d=0.5$, $\sigma_1=\sigma_{-1}=\sigma_0=1$. The snapshots are taken at (a) $t=10\,000$, (b) $t=39\,810$, and (c) $t=100\,000$.

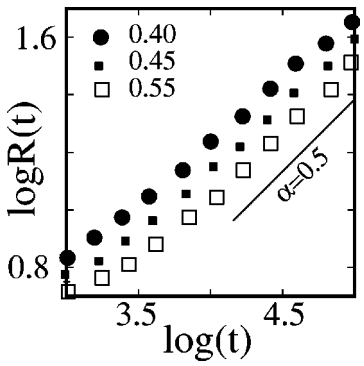

FIG. 10. Variation of c correlation length with $\log_{10}$ (time) in the immiscible three-component case for densities 0.45, 0.5, and 0.55. $\alpha=0.5$ line is given as a guide to the eye.

This implies that R grows with time as $R\sim(vk_BTt/\eta)^{1/2}$ [9].

Another mechanism for droplet coalescence is interfacial diffusion. At nonzero temperatures the domains fluctuate from their circular shape. The area explored by the domain in time t goes as D_bt, where D_b is the diffusion coefficient for the interface. The coalescence time t_c is then given by

$$t_c\sim\frac{R_0^2}{D_b}, \tag{16}$$

here, the length R_0 is such that $\pi R_0^2=$ area of the droplet. Since the interface diffusion coefficient is not a function of R_0, we get $L(t)\sim t^{1/2}$. Thus, both the droplet diffusion and interfacial diffusion could give the same dynamical exponent.

To explore the possibility of the second mechanism, we studied the stability of a drop to fluctuations from the circular shape. As shown in the appendix, in two dimensions, surface fluctuations die out exponentially, both in the case of a drop and a strip [11] of one fluid in another. This implies that in the $\alpha=1/2$ regime, the dominant mechanism for coarsening is the droplet coalescence by diffusion.

Droplet coalescence is the only mechanism operating here and is further confirmed by the existence of scaling. In Fig. 11, we compare the time dependence of the total border

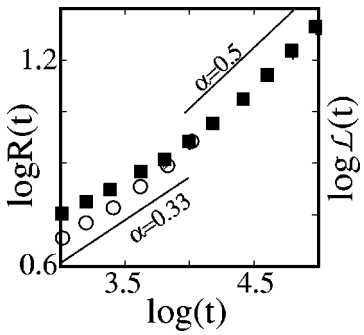

FIG. 11. The first zero of the correlation function R (open circles) and the total border length $\mathcal{L}$ (filled squares) for a symmetric ternary fluid with $\sigma_1=\sigma_{-1}=\sigma_0$ with $\log_{10}$ (time). Average density of the fluids is $d=0.55$. Continuous lines with slopes 1/3 and 1/2 are given as a guide to the eye.

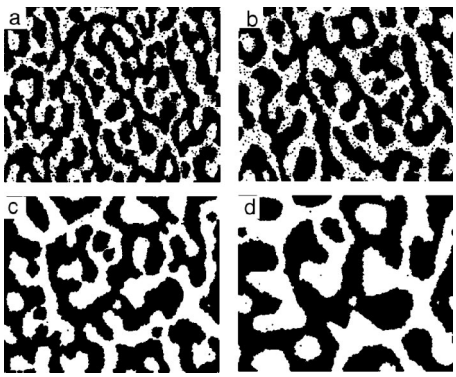

FIG. 12. Time evolution of three-fluid mixture for $d=0.55$. (a) and (b) are the snapshots from the asymmetric ternary mixture phase separation at $t=25\,118$ and $t=39\,810$ with $\sigma_1=\sigma_{-1}=1$ and $\sigma_0=-1.5$. Note the breaking and reorganization of the domains with time. *A*-*C* region is shown in black and *B*-*C* region in white. For comparison, we show snapshots (c) and (d) from the phase separation of a binary mixture having the same density at the same time steps with $\sigma_1=\sigma_{-1}=1$.

length $\mathcal{L}$ of the domains of component *A* with that of the first zero of the correlation function $R(t)$. We observe the same time dependence for both the lengths indicating scaling in the late time regime.

2. Asymmetric case

In this section, we discuss a ternary mixture with one of the components equally soluble in the other two. For this, we choose $\sigma_1=\sigma_{-1}$ and $\sigma_0<-(\sigma_1+\sigma_{-1})$ such that the component $C(i=0)$ is the solute. The components *A* and *B* are mutually immiscible. We choose *A* and *B* to have the same volume fraction. We now have *A*-*C* and *B*-*C* mixtures phase separating similar to the binary fluid under critical quench.

As shown in Fig. 12, the starting mixed phase separates into percolating domains of *A*-*C* and *B*-*C* phases. Though the early time behavior is similar to the two-component fluid with $\sigma_1=\sigma_{-1}$, the late time growth is analogous to the situation, where $\sigma_1\neq\sigma_{-1}$ discussed in Sec. III. The snapshots do not exhibit self-similarity, domains split up and combine during coarsening. In this regime, the first zero of the correlation function exhibits a dynamic exponent $\alpha=1/2$. We would like to point out that for the same density, the two-component fluid with $\sigma_1=\sigma_{-1}$ exhibits a late time exponent $\alpha=2/3$ and does not show any evidence of $\alpha=1/2$ regime. Thus, the third component acts to reduce the interfacial tension between the *A* rich and *B* rich phases leading to fluctuation induced breakup and reorganization of the domains. As the volume fraction of the component *C* is reduced, we observe a gradual change from the $\alpha=1/2$ to $\alpha=2/3$ regime.

In order to investigate the validity of the scaling hypothesis in this regime, we compare the length scales $\mathcal{L}(t)$ and $R(t)$. This is depicted in Fig. 13. It is evident from the figure that these two length scales vary differently at late times.

V. CONCLUSION

We have presented the dynamics of domain growth in binary and ternary immiscible fluids, using a two-dimensional hydrodynamic lattice-gas model. Various dynamic regimes are investigated by altering parameters like volume fraction, the interaction strength of the individual components, and a temperature like variable.

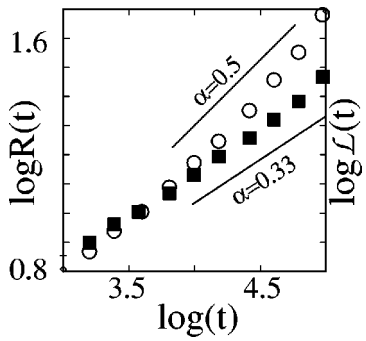

FIG. 13. The first zero of the correlation function (open circles) and the total border length (filled squares) in three-component asymmetric fluids with $\log_{10}$ (time). Continuous lines with slopes 0.33 and 0.5 are given as reference.

We examine the validity of scaling in two-component fluid coarsening by comparing the dynamic nature of the first zero of the correlation function and the total border length. While scaling holds in the droplet coalescence and the inertial hydrodynamic regimes, violation of scaling is observed in the fluctuation dominated regime.

In symmetric ternary mixtures, we show the existence of a coalescence dominated regime with a single length scale exhibiting a dynamical exponent $\alpha=1/2$. In asymmetric ternary mixtures we use the concentration of the solute as a control parameter. We demonstrate that at higher solute concentrations, the coarsening is driven by fluctuations and scaling is violated.

APPENDIX

Stability of the drop

In this Appendix, we look at the stability of a drop with radius *R* against perturbations in its perimeter. We consider a drop of radius *R* with the fluid in the region $r<R$ characterized by density ρ, and kinematic viscosity $\nu=\eta/\rho$ surrounded by another fluid with density ρ' and kinematic viscosity ν'. For an incompressible and vorticity free fluid, we can define the velocity component using a streaming potential ψ as $v_r=(1/r)(\partial\psi/\partial\phi)$, $v_\phi=-\partial\psi/\partial r$.

Navier-Stokes equation then reduces to

$$(\partial_t-\nu\nabla^2)\nabla^2\psi(r,\phi,t)=0. \tag{A1}$$

We look for solutions of the form $\psi(r,\phi,t)=\psi_1(r,\phi,t)+\psi_2(r,\phi,t)$ such that

$$\nabla^2\psi_1=0, \tag{A2}$$

$$(\partial_t-\nu\nabla^2)\nabla^2\psi_2(r,\phi,t)=0. \tag{A3}$$

The general solutions of these equations in cylindrical polar coordinates is

$$\psi_1(r,\phi,t)=\left(a_m r^m+\frac{b_m}{r^m}\right)e^{im\phi}e^{\omega t}, \tag{A4}$$

$$\psi_2(r,\phi,t)=[\alpha_m I_m(kr)+\beta_m K_m(kr)]e^{im\phi}e^{\omega t}, \tag{A5}$$

where $k=(\omega/\nu)^{1/2}$ and $I_m(kr)$ and $K_m(kr)$ are modified Bessel functions.

The coefficients a_m, b_m, α_m, and β_m are obtained from the four equations; the continuity of v_r at $r=R$, continuity of v_ϕ at $r=R$, continuity of tangential stress $\sigma_{r\phi}$ at $r=R$ and the relation between normal stresses

$$\sigma_{rr}|_{r=R^-}+p^-=\sigma_{rr}|_{r=R^+}+p^++p_\sigma. \tag{A6}$$

For the pressure p, we write $P=p(r)e^{im\phi}e^{\omega t}$. The pressure due to surface tension is obtained from the Young Laplace formula

$$P_\sigma=\frac{\sigma i m^3}{R_0^3\omega}\psi_{r<R}. \tag{A7}$$

These equations can be written in a matrix form

$$\begin{bmatrix} R^m & -1/R^m & I_m & -K_m \\ R^{m-1} & 1/R^{m+1} & -I_m/R+\frac{k}{m}I_{m-1} & -K_m/R+\frac{k}{m}K_{m-1} \\ -2(m^2+m)R^{m-2} & \frac{2(m^2+m)}{R^{m+2}} & A_{33} & A_{34} \\ A_{41} & A_{42} & A_{43} & A_{44} \end{bmatrix}\begin{bmatrix} a_m \\ b_m \\ \alpha_m \\ \beta_m \end{bmatrix}=0, \tag{A8}$$

where

$$A_{33}=-\left(\frac{k^2}{2}+\frac{2m}{R^2}+\frac{m^2}{R^2}\right)I_m+\frac{mk}{2R}I_{m+1}+\left(\frac{mk}{2R}+\frac{k}{R}\right)I_{m-1}-k^2I_{m-2},$$

$$A_{34}=\left(\frac{k^2}{2}+\frac{2m}{R^2}+\frac{m^2}{R^2}\right)K_m+\frac{mk}{2R}K_{m+1}+\left(\frac{mk}{2R}+\frac{k}{R}\right)K_{m-1}+k^2K_{m-2},$$

$$A_{41}=\nu\left(2m^2+k^2R^2-1+\frac{\sigma m^3}{R\omega\eta}\right)R^{m-2},$$

$$A_{42}=\frac{\nu(2m^2+k^2R^2-1)}{R^{(m+2)}},$$

$$A_{43}=\nu\left[\left(\frac{2m^2}{R^2}-\frac{4m}{R^2}+\frac{1}{R^2}+\frac{\sigma m^3}{R^3\omega\eta}\right)I_m-\frac{k}{mR}(1-2m)I_{m-1}+\frac{2k}{R}(m-1)I_{m-1}\right],$$

$$A_{44}=\nu\left[\left(-\frac{2m^2}{R^2}+\frac{4m}{R^2}-\frac{1}{R^2}\right)K_m-\frac{k}{mR}(1-2m)K_{m-1}+\frac{2k}{R}(m-1)K_{m+1}\right]. \tag{A9}$$

In the limit of large viscosity, we can neglect all terms of order $\sqrt{(\omega/\eta)}$. The condition for nontrivial solutions in this limit leads to a relation between ω and m;

$$\omega=\frac{m^3\sigma}{(1-4m^2)R\eta}. \tag{A10}$$

Since the right hand side of this equation is always negative, we come to the conclusion that in the limit of high viscosity there are no unstable modes. In the more general case, the condition for nontrivial solutions leads to a transcendental equation for ω and m. A numerical analysis on this equation does not yield any unstable solutions.

[1] N.C. Wong and C.M. Knobler, Phys. Rev. A **24**, 3205 (1981).
[2] Y.C. Chou and W.I. Goldburg, Phys. Rev. A **23**, 858 (1981).
[3] F. Perrot, D. Guenoun, T. Baumberger, D. Beysens, Y. Garrabos, and B. LeNeindre, Phys. Rev. Lett. **73**, 688 (1994).
[4] S. Walheim, M. Ramstein, and U. Steiner, Langmuir **15**, 4828 (1999).
[5] E. Valasco and S. Toxvaerd, Phys. Rev. Lett. **71**, 388 (1993).
[6] G. Leptoukh, B. Strickland, and C. Roland, Phys. Rev. Lett.

74, 3636 (1995).
[7] O.T. Valls and James E. Farrell, Phys. Rev. B **40**, 7027 (1989).
[8] A.J. Bray, Adv. Phys. **43**, 557 (1994).
[9] E.D. Siggia, Phys. Rev. A **20**, 595 (1973).
[10] H. Furukawa, Physica A **204**, 237 (1994).
[11] M. San Miguel, M. Grant, and J.D. Gunton, Phys. Rev. A **31**, 1001 (1985).
[12] A.J. Wagner and J.M. Yeomans, Phys. Rev. Lett. **80**, 1429 (1998).
[13] H. Tanaka, Phys. Rev. Lett. **72**, 1702 (1994).
[14] A.J. Wagner and M.E. Cates, Europhys. Lett. **56**, 556 (2001).
[15] H. Furukawa, Phys. Rev. E **61**, 1423 (2000).
[16] I. Pagonobaraga, A.J. Wagner, and M.E. Cates, J. Stat. Phys. (to be published).
[17] M.R. Swift, E. Orlandini, W.R. Osborn, and J.M. Yeomans, Phys. Rev. E **54**, 5041 (1996).
[18] F.J. Alexander, S. Chen, and D.W. Grunau, Phys. Rev. B **48**, 634 (1993).
[19] A.J. Wagner and J.M. Yeomans, Int. J. Mod. Phys. C **9**, 1373 (1998).
[20] D.H. Rothmann and J.M. Keller, J. Stat. Phys. **2**, 1119 (1988).
[21] S. Bastea and J.L. Lebowitz, Phys. Rev. E **52**, 3821 (1995).
[22] A.N. Emerton, P.V. Coveney, and B.M. Boghosian, Phys. Rev. E **55**, 708 (1997).
[23] T. Kawakatsu *et al.*, J. Chem. Phys. **99**, 8200 (1993).
[24] G. Gonnella *et al.*, Phys. Rev. E **58**, 480 (1998).
[25] M. Laradji, O.G. Mouritsen, and S. Toxvaerd, Europhys. Lett. **28**, 157 (1994).
[26] A.K. Gunstensen and D.H. Rothman, Physica D **47**, 47 (1990).
[27] K.A. Smith *et al.*, Phys. Rev. Lett. **84**, 91 (2000).
[28] B. Chopard and M. Droz, *Cellular Automata Modeling of Physical Systems* (Cambridge University Press, Cambridge, 1998).